Pramāṇa, Vol. 15, No. 5, November 1980, pp. 435–447. © Printed in India.

High spin yrast states in even platinum isotopes

ASHOK KUMAR and M R GUNYE
Theoretical Reactor Physics Section, Bhabha Atomic Research Centre, Trombay, Bombay 400 085, India

MS received 7 June 1980; revised 12 September 1980

Abstract. The high spin yrast states up to $J = 20^+$ in ^{184}, ^{186}Pt and ^{190}, ^{192}, ^{194}Pt are studied in a microscopic approach of variation with number-conserved projected states. The energy spectra, quadrupole moments and $B(E2)$ values are calculated by employing the Hamiltonian with quadrupole plus pairing interactions. The results of the calculations are in fair agreement with the available experimental data.

Keywords. Nuclear structure; platinum isotopes; energy spectra; quadrupole moments; $B(E2)$ values.

1. Introduction

The nuclei of tungsten, osmium and platinum form an important region of transition from the deformed rare-earth nuclei to the spherical ^{208}Pb and for this reason are of special interest in testing the predictions of different nuclear models. These transition nuclei provide a probe for studying the details of nuclear collective motion. The collective properties of the low-lying states of the heavy transitional nuclei are investigated (Davydov and Fillipov 1958; Davydov and Chaban 1960; Das Gupta and Gunye 1963; Faessler *et al* 1965) in various collective models developed on the basis of different equilibrium shapes for these nuclei. Extensive theoretical studies on the equilibrium deformations of the transition nuclei have been carried out in the framework of the Nilsson model by incorporating pairing correlations (Gunye *et al* 1964) and the quadrupole plus pairing model (Kumar and Baranger 1968). The nuclear shape changes from prolate to oblate in the mass region $A \sim 188$ (Gunye *et al* 1964; Kumar and Baranger 1968). Thus the nuclei $^{184-186}$Pt have prolate shape, ^{188}Pt is axially asymmetric whereas ^{190,192,194}Pt prefer an oblate equilibrium shape (Kumar and Baranger 1968). Nuclear structure studies, both experimental and theoretical, in osmium and platinum nuclei are being pursued with great interest in recent years. The back-bending phenomenon observed (Sorensen 1973; Johnson and Szymanski 1973) in some deformed rare-earth nuclei gave a stimulus to investigate high spin states in heavy nuclei. Recent experiments have established (Hjorth *et al* 1976; Cunnane *et al* 1976; Johnson *et al* 1977; Beshai *et al* 1976; Piiparinen *et al* 1975) the energy spectra of even platinum isotopes up to high spin states with $J \leqslant 20$. A pronounced back-bending at the critical angular momentum $J_c = 10$ is observed in the yrast band of ^{190,192,194}Pt isotopes. The analysis of the available data on the low-lying states in ^{194}Pt indicates (Baktash *et al* 1978) that the quadrupole plus pairing force model is favoured over the triaxial rigid ro-

tator model. The aim of this paper is to see whether the quadrupole plus pairing force model which ascribes prolate equilibrium shapes to ^{184,186}Pt and oblate equilibrium shapes to ^{190,192,194}Pt can explain the observed characteristics of their energy spectra of the yrast band.

The anomalous back-bending behaviour in the rotational band is interpreted as a manifestation of the Coriolis interaction between the collective and intrinsic motion of nucleons. There are two alternative proposals to explain the anomalous behaviour in terms of the Coriolis force. Mottelson and Valatin (1960) attribute this anomalous behaviour to the Coriolis antipairing phase transition from the superfluid to the normal nuclear state. The alternative proposal by Stephens and Simon (1972) states that certain individual nucleons may respond to the Coriolis force prior to the phase transition proposed by Mottelson and Valatin (1960). The rotation alignment proposal of Stephens and Simon (1972) attributes back-bending to the Coriolis decoupling of a nucleon pair in orbital with high angular momentum j from the rotating core and subsequent alignment with the core angular momentum. The Coriolis force is strong if the Fermi surface is close to the substates of high-j states with small projection Ω on the symmetry axis and under such circumstances, the decoupled band can drop below the completely paired normal band at higher spins, thus causing back-bending. It thus seems that the single-particle orbitals with low Ω and high j near the Fermi surface play an important role in the anomalous effect occurring at some critical angular momentum.

It is of interest to gain an insight into the intrinsic structure of the high spin states from a microscopic theory. Some attempts (Faessler *et al* 1974, Warke and Gunye 1975, 1976) are made in this direction to understand the structure of high spin states in the framework of the many-body variational formalism with good angular momentum. Apart from the complication of angular momentum projection in a large configuration space, there is yet another complication due to number projection (Grummer *et al* 1975; Gunye and Warke 1979) from the pair-correlated variational state. It is found (Gunye and Warke 1979) that the number conservation in each projected state improves the quality of the agreement between theoretical and experimental results. In this paper, we report the results of the microscopic calculations on the yrast states of ^{184,186}Pt and ^{190,192,194}Pt nuclei. The details of the calculations, performed in a variational formulation with angular momentum projection by conserving the nucleon numbers in each projected state, are given in §2 The results are discussed in §3 and the conclusions in §4.

2. Details of calculation

A realistic nuclear structure calculation in a microscopic many-body formalism requires treatment of a large number of nucleons in a large configuration space. The computational difficulties involved in such a realistic calculation can be reduced by employing a simpler many-body Hamiltonian. In this paper, we use the quadrupole plus pairing interaction Hamiltonian,

$$H = \sum \epsilon_\alpha a_\alpha^+ a_\alpha - \tfrac{1}{2}\chi \sum q_{\alpha\gamma}^{\mu} q_{\delta\beta}^{\mu} a_\alpha^+ a_\beta^+ a_\delta a_\gamma - \tfrac{1}{2} G \sum (-)^{j_\alpha - m_\alpha + j_\gamma - m_\gamma} a_\alpha^+ a_{\bar{\alpha}}^+ a_{\bar{\gamma}} a_\gamma, \quad (1)$$

where q^{μ} is the quadrupole operator and χ and G are the strengths of quadrupole and pairing interactions respectively. The subscript α in (1) denotes all the quantum numbers $(n_\alpha, l_\alpha, j_\alpha, m_\alpha)$ necessary for the specification of a single-particle state with energy ϵ_α. The parameters of this Hamiltonian in (1) are determined by Kumar and Baranger (1968) from the study of equilibrium deformation of heavy nuclei and we use their values in the present calculations. The intrinsic variational wavefunction is assumed to be axially symmetric in view of the fact that the nuclei under investigation are found (Kumar and Baranger 1968) to prefer axially symmetric equilibrium deformation. We have, however, not performed the calculations for ^{188}Pt which is an axially asymmetric nucleus. The nuclear structure calculations in this nucleus ^{188}Pt are recently carried out by Sahu *et al* (1979) by a variational method of approximate angular momentum projection from a triaxial intrinsic wavefunction.

The trial wavefunction is taken to be the good angular momentum state $\Psi^J_M(\beta, \Delta_p, \Delta_n, \lambda_p, \lambda_n)$ projected from the intrinsic BCS state $\Phi_o(\beta, \Delta_p, \Delta_n, \lambda_p, \lambda_n)$. The deformation β, the pairing gaps Δ_p and Δ_n and the chemical potentials λ_p and λ_n are the variational parameters for each angular momentum state J. The suffixes p and n refer to proton and neutron respectively. The nuclear energy E^J in the state J is calculated by minimising the expectation value of the Hamiltonian in (1) in the projected state Ψ^J_M (Warke and Gunye 1976). The energy minima are found by varying the parameters β, Δ_p, Δ_n, λ_p and λ_n simultaneously. For each set of values of β, Δ_p and Δ_n, the chemical potentials λ_p and λ_n are varied so as to yield the correct number Z of protons and N of neutrons for each angular momentum state J. The calculated number of nucleons are very sensitively dependent on λ_p and λ_n and it is, therefore, necessary to incorporate very fine variations of λ_p and λ_n in the variational procedure so as to obtain the correct number in each angular momentum state. In the present calculations, we have achieved an accuracy up to the fourth decimal place in the nucleon numbers in each state.

The values of the strength parameters χ and G are estimated by Kumar and Baranger (1968) in a truncated configuration space of two major shells each for protons and neutrons by assuming an inert core with $Z=40$ and $N=70$. The assumption of an inert core necessitates the modification of the nucleon charges and excitation energies. As is the standard practice (Kumar and Baranger 1968), we replace the bare nucleon charges by effective charges to simulate the effects of core-polarisation and configuration truncation. The simplest way to incorporate the effect of the neglected core on the projected energies is by renormalising the calculated energy spectra. We achieve it by introducing a parameter, namely the moment of inertia I_{core} of the core. The moment of inertia of the nucleus is assumed to be the sum of the moment of inertia I_{core} of the core and I_{calc} of the outer nucleons. The energy E^J_{calc}, computed by considering only the outer valence nucleons can be expressed as

$$E^J_{\text{calc}} = J(J+1)\frac{\hbar^2}{2\,I_{\text{calc}}} \tag{2}$$

and similarly, the corrected or the renormalised energy can be expressed as

$$E^J_{\text{norm}} = J(J+1)\frac{\hbar^2}{2\,(I_{\text{core}}+I_{\text{calc}})} = E^J_{\text{calc}}\left(\frac{I_{\text{calc}}}{I_{\text{core}}+I_{\text{calc}}}\right). \tag{3}$$

Since the calculated energy E^J_{calc} deviates from the pure rotational pattern, the moment of inertia I_{calc} varies with the angular momentum J. The moment of inertia I_{core} may either be a constant, at least for a set of states, or may vary with J. If I_{core} and I_{calc} vary with J in a similar manner, the ratio $I_{\text{calc}}/(I_{\text{core}}+I_{\text{calc}})$ in (3) would remain constant.

3. Results and discussion

It has been found (Kumar and Baranger 1968) that a prolate equilibrium shape is preferred for ^{184,186}Pt nuclei while the nuclei ^{190,192,194}Pt prefer an oblate equilibrium shape. For convenience we discuss their results separately.

3.1 *The prolate nuclei ^{184,186}Pt*

The calculated energy spectra in both the nuclei ^{184,186}Pt are renormalised by choosing a suitable value of the parameter I_{core}. As discussed in § 2, the value I_{core} may either be a constant or vary with J. In these two prolate nuclei, we find that an overall agreement with the experimental energy spectra can be obtained by choosing a constant value of the parameter I_{core}. We have employed the value $I_{\text{core}}=14\hbar^2/\text{MeV}$ for renormalisation of the energy spectra calculated from the variational microscopic calculations. The renormalised energy and the variational parameters β, Δ_p, and Δ_n corresponding to the minimum of energy for each angular momentum state J are shown in tables 1 and 2 for ^{184}Pt and ^{186}Pt respectively. It is seen that the renormalised energies in both the nuclei are in good agreement with the corresponding experimental values, the maximum deviation being less than 100 keV for all the states except for $J=20$ in the case of ^{184}Pt where the deviation is

Table 1. The deformation β, the pairing gaps Δ_p and Δ_n, the energy E_{norm} obtained from the renormalisation procedure, the experimental energy E_{exp}, the quadrupole moment $Q(J)$ and the $B(E2; J\to J-2)$ value for each angular momentum state J in ^{184}Pt. The number in bracket indicates the corresponding experimental value.

J	β	Δ_p (MeV)	Δ_n (MeV)	E_{norm} (MeV)	E_{exp} (MeV)	$-Q(J)$ (eb)	$B(E2; J\to J-2)$ (e^2b^2)
0	0·20	0·75	0·95	0·00	0·00		
2	0·20	0·75	0·95	0·13	0·16	1·30	0·53 (0·78 ± 0·04)†
4	0·23	0·79	0·84	0·39	0·44	1·65	0·60
6	0·23	0·79	0·59	0·78	0·80	1·83	0·67
8	0·23	0·79	0·33	1·24	1·23	1·94	0·72
10	0·23	0·79	0·00	1·71	1·73	1·97	0·75
12	0·23	0·79	0·00	2·19	2·23	2·04	0·76
14	0·20	0·75	0·00	2·73	2·75	1·90	0·65
16	0·20	0·75	0·00	3·32	3·30	1·89	0·66
18	0·20	0·75	0·00	3·97	3·89	1·89	0·67
20	0·20	0·75	0·00	4·67	4·52	1·88	0·68

†Richter *et al* (1979)

Table 2. The deformation β, the pairing gaps Δ_p and Δ_n, the energy E_{norm} obtained from the renormalisation procedure, the experimental energy E_{exp}, the quadrupole moment $Q(J)$ and the $B(E2; J \rightarrow J-2)$ value for each angular momentum state J in ^{186}Pt. The number in bracket indicates the corresponding experimental value.

J	β	Δ_p (MeV)	Δ_n (MeV)	E_{norm} (MeV)	E_{exp} (MeV)	$-Q(J)$ (eb)	$B(E2; J \rightarrow J-2)$ (e^2b^2)
0	0·20	0·73	0·94	0·00	0·00		
2	0·20	0·73	0·94	0·13	0·19	1·16	0·43 (0·59 ± 0·03)†
4	0·23	0·77	0·84	0·42	0·49	1·64	0·59
6	0·23	0·77	0·59	0·82	0·88	1·81	0·67
8	0·23	0·77	0·34	1·30	1·34	1·92	0·71
10	0·23	0·77	0·00	1·80	1·86	1·99	0·74
12	0·23	0·77	0·00	2·34	2·34	2·02	0·76
14	0·20	0·73	0·00	2·93	2·83	1·87	0·66
16	0·20	0·73	0·00	3·60	—	1·87	0·67
18	0·20	0·73	0·00	4·34	—	1·86	0·68
20	0·20	0·73	0·00	5·15	—	1·85	0·69

†Richter *et al* (1979)

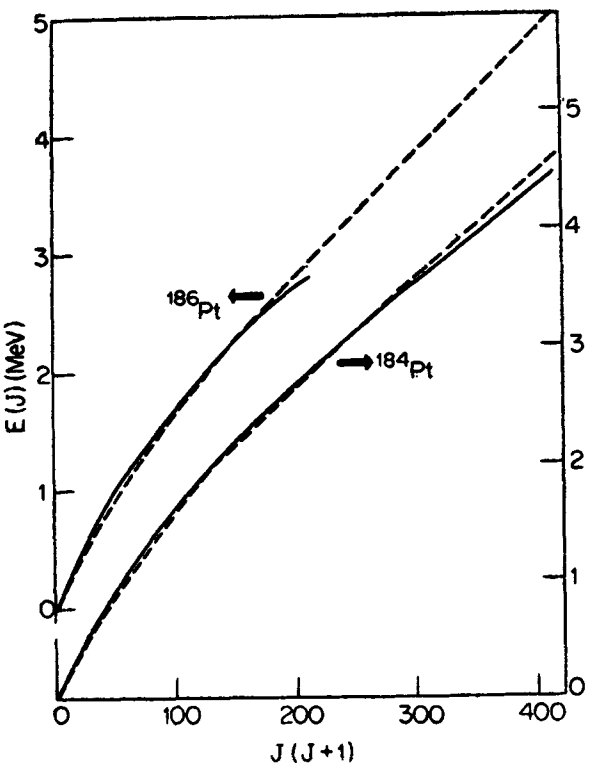

Figure 1. The calculated (dashed curve) and the experimental (solid curve) values of the energy $E(J)$ for each angular momentum state J in ^{184}Pt (right) and ^{186}Pt (left) are plotted as a function of $J(J+1)$.

150 keV. In order to visualise the agreement between the calculated and experimental energy spectra at a glance, we have plotted the energy $E(J)$ as a function of $J(J+1)$ for the nuclei ^{184,186}Pt in figure 1. This plot brings out the salient feature of a departure of the energy spectra from the simple rotational structure based on a single band. The back-bending behaviour is conventionally illustrated by the familiar S-shaped curve by plotting the moment of inertia I as a function of square of rotational frequency ω for each angular momentum state J. It should be stressed here that the calculated energies should be in very precise agreement with the experimental energies so as to reproduce the characteristic experimental S curve. Since the microscopic calculations with the simple quadrupole-plus-pairing force model cannot yield such precise agreement, one can only expect to see the trend of the I vs ω^2 curve. The theoretical and experimental back-bending curves for ^{184}Pt are shown in figure 2.

It is seen from the results shown in tables 1 and 2 that the deformation β for both the nuclei ^{184,186}Pt is same ($\beta=0{\cdot}20$) for all the yrast states except those with $4 \leqslant J \leqslant 12$ for which it assumes a larger value ($\beta=0{\cdot}23$). The pairing gap Δ_p for protons remains almost the same for all the yrast states up to $J=20$ in both the nuclei. The situation in the corresponding case of neutrons is, however, quite different. The pairing gap Δ_n for neutrons in both the nuclei remains nearly the same for the yrast states up to $J=4$ and then decreases smoothly with the increase in J until it vanishes at $J=10$ so as to remain zero for all higher states with $J \geqslant 10$. Thus the observed back-bending in these nuclei at a critical angular momentum $J_c=10$ can be due to the vanishing of the neutron pairing gap Δ_n at $J=10$. We have plotted in figure 3 the pairing gaps Δ_p and Δ_n as a function of J for both the nuclei to illustrate this point.

The back-bending in a given nucleus would also depend in detail on the structure

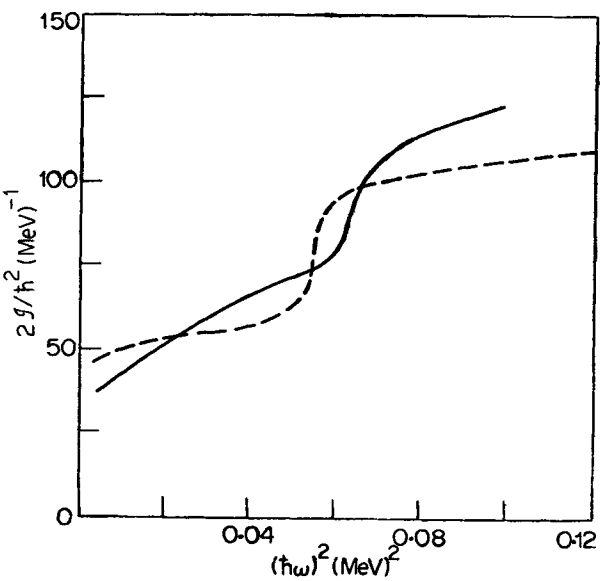

Figure 2. The calculated (dashed) and the experimental (solid) curves of the moment of inertia as a function of the square of the rotational frequency are plotted in the case of ^{184}Pt.

of single-particle orbitals near the Fermi surface of protons and neutrons. The phenomenological approach of Stephens and Simon (1972) is based on decoupling of bands where the Coriolis effects in high-j single-particle orbitals near the Fermi surface play an important role. We find that in the range of deformation relevant for these nuclei there is no orbital of high-j with low-Ω near the proton Fermi surface. As regards the neutron states, the only high-j orbital near the neutron Fermi surfaces of both the nuclei in the relevant range of deformation is the $\Omega = 9/2$ substate, predominantly from the $i_{13/2}$ state. Since the Coriolis force is weak for high Ω substates, the back-bending probably cannot result from a decoupling of a neutron pair in this $i_{13/2}$ orbit near the neutron Fermi surface.

3.2 *The oblate nuclei* ^{190,192,194}Pt

The calculated energy spectra in these nuclei are renormalised by introducing the parameter I_{core} as discussed in § 2. The moment of inertia I_{core} may either be a constant, at least for a set of states, or may vary with J. In these oblate nuclei, we find that for the states with $J \geqslant 12$, an overall agreement with the experimental energy spectra can be obtained by choosing a constant value $I_{\text{core}} = 14{\cdot}5\ \hbar^2/\text{MeV}$. We find, however, that for $J \leqslant 10$, the value I_{core} varies with J keeping the ratio $I_{\text{calc}}/(I_{\text{core}} + I_{\text{calc}})$ nearly constant for all the yrast states with $4 \leqslant J \leqslant 10$. The value of this ratio is, however, slightly larger for $J = 2^+$ states in these platinum isotopes. We have renormalised the calculated energy spectra of all the three oblate platinum nuclei by fixing the ratio $I_{\text{calc}}/(I_{\text{core}} + I_{\text{calc}})$ so as to reproduce the observed excitation energy of $J = 6$ yrast state in each nucleus. To obtain a more accurate energy of 2^+ yrast states, one may have to take into account the interaction between the oblate and prolate intrinsic states.

The renormalised energy and the variational parameters β, Δ_p and Δ_n corresponding to the minimum of energy for each angular momentum state J are shown in tables 3, 4 and 5 for ^{190}Pt, ^{192}Pt and ^{194}Pt respectively. It can be seen from these

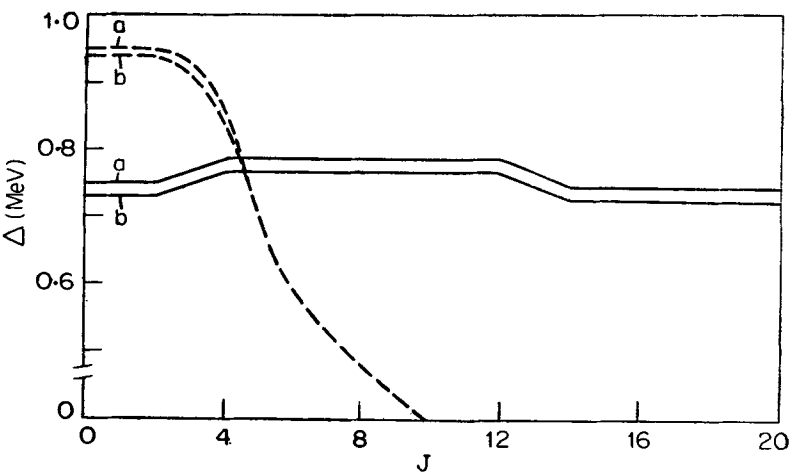

Figure 3. The pairing gaps Δ_p for protons (solid curve) and Δ_n for neutrons (dashed curve) corresponding to the minimum in energy are plotted as function of angular momentum J. The curves a and b refer to ^{194}Pt and ^{196}Pt respectively.

tables that the renormalised energies are in fair agreement with the corresponding experimental energies, the maximum deviation being about 130 keV in ^{190,192}Pt and about 200 keV in ^{194}Pt. In order to visualise the agreement between the calculated and the experimental energy spectra at a glance we have plotted the energy $E(J)$ as a function of $J(J+1)$ in figure 4 for ^{190,192}Pt. These plots clearly bring out the salient feature of the departure of the energy spectra from the simple rotational picture based on a single band. The drastic change in the slope of the curves $E(J)$ vs $J(J+1)$ at $J=10$ in figure 4 indicates the anomalous back-bending observed in the energy spectra of the yrast states in these nuclei. As this back-bending behaviour is conventionally illustrated by the I vs ω^2 plot, we have plotted in figure 5 the theoretical and experimental back-bending curves in ^{190}Pt for comparison. Since the microscopic calculations with the simple quadrupole-plus-pairing force model cannot yield precise agreement in energy of each individual state, one should expect to see only the trend of the I vs ω^2 curve.

It is seen from the results shown in tables 3, 4 and 5 that the deformation β is the same ($\beta=-0{\cdot}18$ in ^{190,192}Pt and $\beta=-0{\cdot}16$ in ^{194}Pt) for all the yrast states except those with $4 \leqslant J \leqslant 8$ for which it is large in magnitude by 0·02. It should be mentioned here that the deformation corresponding to the energy minimum of the projected $J=0$ ground state in all ^{190,192,194}Pt isotopes is slightly larger in magnitude than that obtained (Kumar and Baranger 1968) from the energy minimum of the intrinsic state of the nuclei.

In all the three platinum nuclei under investigation, the pairing gap Δ_p for protons remains nearly constant for all the yrast states, as seen from tables 3, 4 and 5. The neutron pairing gap Δ_n, however, remains nearly constant for the first three yrast states with $J \leqslant 4$ and then decreases with increasing J till it vanishes suddenly

Table 3. The deformation β, the pairing gaps Δ_p and Δ_n, the energy E_{norm} obtained from the renormalisation procedure, the experimental energy E_{exp}, the quadrupole moment $Q(J)$ and the $B(E2; J \rightarrow J-2)$ value for each angular momentum state J in ^{190}Pt. The numbers in bracket indicate the corresponding experimental values.

J	β	Δ_p (MeV)	Δ_n (MeV)	E_{norm} (MeV)	E_{exp} (MeV)	$Q(J)$ (eb)	$B(E2; J \rightarrow J-2)$ (e^2b^2)
0	−0·18	0·65	1·04	0·00	0·00		
2	−0·18	0·65	1·04	0·20	0·30	1·17	0·42 (0·49 ± 0·14)†
4	−0·20	0·63	0·98	0·69	0·74	1·64	0·59
6	−0·20	0·63	0·69	1·29	1·29	1·82	0·66
8	−0·20	0·63	0·69	1·88	1·92	1·91	0·72
10	−0·18	0·65	0·00	2·41	2·54	1·98	0·74
12	−0·18	0·65	0·00	2·65	2·73	1·87	0·63 (>0·22)†† (~0·11)*
14	−0·18	0·65	0·00	3·13	3·07	1·90	0·64
16	−0·18	0·65	0·00	3·65	3·58	1·92	0·65
18	−0·18	0·65	0·00	4·19	4·21	1·93	0·66
20	−0·18	0·65	0·00	4·76	—	1·94	0·67

†Richter *et al* (1979)
††Hjorth *et al* (1976)
*Piiparinen *et al* (1975)

Table 4. The deformation β, the pairing gaps Δ_p and Δ_n, the energy E_{norm} obtained from the renormalisation procedure, the experimental energy E_{exp}, the quadrupole moment $Q(J)$ and the $B(E2; J \rightarrow J-2)$ value for each angular momentum state J in ^{192}Pt. The numbers in bracket indicate the experimental values.

J	β	Δ_p (MeV)	Δ_n (MeV)	E_{norm} (MeV)	E_{exp} (MeV)	$Q(J)$ (eb)	$B(E2: J \rightarrow J-2)$ (e^2 b^2)
0	−0·18	0·64	0·98	0·00	0·00		
2	−0·18	0·64	0·98	0·26	0·32	1·16	0·34 (0·34 ± 0·02)†
4	−0·18	0·64	0·98	0·71	0·79	1·48	0·49 (0·58 ± 0·03)†
6	−0·20	0·61	0·65	1·37	1·37	1·80	0·63 (0·47 ± 0·18)†
8	−0·20	0·61	0·65	1·99	2·02	1·91	0·72
10	−0·18	0·64	0·00	2·42	2·52	1·79	0·57
12	−0·18	0·64	0·00	2·64	2·62	1·82	0·58 (1·62 ± 0·26)† (~0·27)††
14	−0·18	0·64	0·00	3·14	3·00	1·85	0·62
16	−0·18	0·64	0·00	3·66	3·54	1·87	0·63
18	−0·18	0·64	0·00	4·20	4·20	1·88	0·64
20	−0·18	0·64	0·00	4·93	4·95	1·90	0·64

†Johnson *et al* (1977)
††Piiparinen *et al* (1975)

Table 5. The deformation β, the pairing gaps Δ_p and Δ_n, the energy E_{norm} obtained from the renormalisation procedure, the experimental energy E_{exp}, the quadrupole moment $Q(J)$ and the $B(E2: J \rightarrow J-2)$ value for each angular momentum state J in ^{194}Pt. The numbers in bracket indicate the corresponding experimental values.

J	β	Δ_p (MeV)	Δ_n (MeV)	E_{norm} (MeV)	E_{exp} (MeV)	$Q(J)$ (eb)	$B(E2: J \rightarrow J-2)$ (e^2 b^2)
0	−0·16	0·65	0·91	0·00	0·00		
2	−0·16	0·65	0·91	0·20	0·33	1·08 (0·63 ± 0·06)†	0·29 (0·32 ± 0·03)††
4	−0·18	0·62	0.86	0·73	0·81	1·52 (0·5 ± 1·0)†	0·52 (0·47 ± 0·14)††
6	−0·18	0·62	0·60	1·41	1·41	1·68	0·58 (0·48 ± 0·14)††
8	−0·18	0·62	0·60	2·09	2·10	1·77	0·62 (0·36 ± 0·11)††
10	−0·16	0·65	0·00	2·24	2·44	1·62	0·49
12	−0·16	0·65	0·00	2·64	2·83	1·67	0·51
14	−0·16	0·65	0·00	2·91	—	1·73	0·54
16	−0·16	0·65	0·00	3·33	—	1·76	0·54
18	−0·16	0·65	0·00	3·98	—	1·78	0·54
20	−0·16	0·65	0·00	4·90	—	1·80	0·55

†Baktash *et al* (1978)
††Stelzer *et al* (1977)

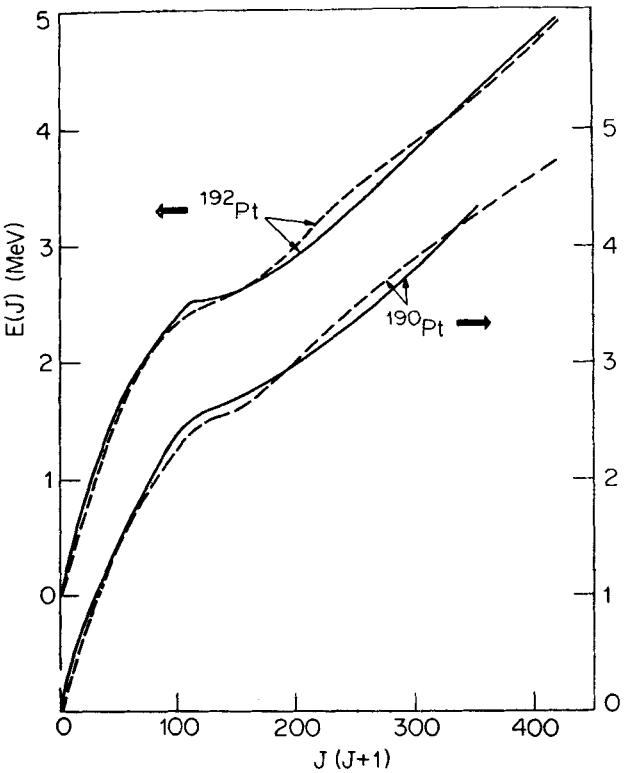

Figure 4. The calculated (dashed curve) and the experimental (solid curve) values of the energy $E(J)$ for each angular momentum state J in ^{190}Pt (right) and ^{192}Pt (left) are plotted as a function of $J(J+1)$.

at $J=10$, remaining zero for all the higher spin states. The plots of the pairing gaps Δ_p and Δ_n as a function of J for all the three nuclei are shown in figure 6. The drastic back-bending observed in these nuclei ^{190,192,194}Pt at the critical angular momentum $J_c=10$ can thus be due to the sudden vanishing of the neutron pairing gap Δ_n at $J=10$.

In view of the fact that these ^{190,192,194}Pt isotopes exhibit a sharp back-bending at a critical angular momentum $J_c=10$, it is worthwhile to mention the single-particle states at the Fermi surface of nucleons since the back-bending also depends in detail on the structure of these single-particle orbitals near the Fermi surface of protons and neutrons. We find that there is no orbital of high-j near the proton Fermi surface of the nuclei ^{190,192,194}Pt. However, the situation in the vicinity of the neutron Fermi surface in the region of deformation relevant for these nuclei is quite different. The substates $\Omega=1/2$ and $\Omega=3/2$ from predominantly $i_{13/2}$ orbital are quite close to the neutron Fermi surface of these nuclei. Since the Coriolis force is strong for low Ω substates of high j orbitals near the Fermi surface, the decoupling of a neutron pair from these low Ω substates of $i_{13/2}$ orbit can give rise to the observed back-bending at the critical angular momentum in the three platinum nuclei ^{190,192,194}Pt.

The quadrupole moment $Q(J)$ and the $B(E2;\ J\rightarrow J-2)$ values in all the nuclei of platinum under consideration are calculated by employing the number-conserved

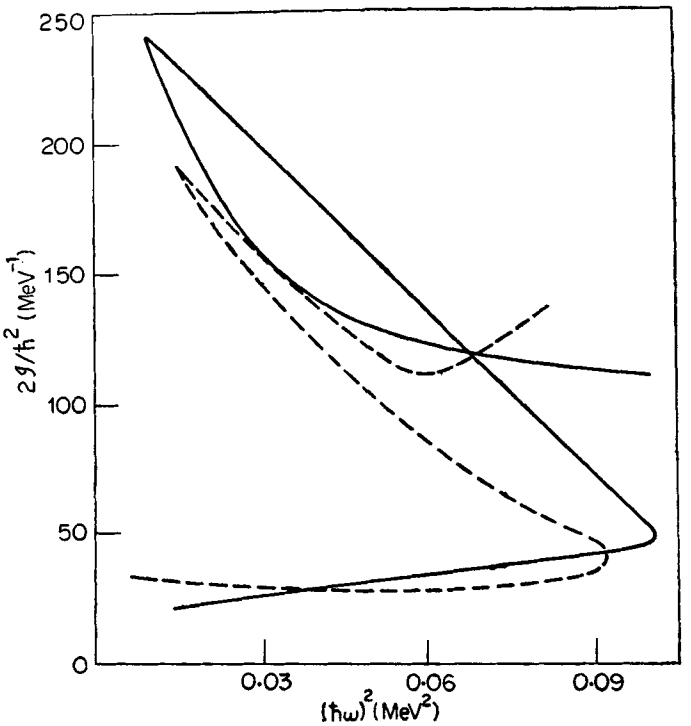

Figure 5. The calculated (dashed) and the experimental (solid) curves of the moment of inertia as a function of square of the rotational frequency are plotted in the case of ^{190}Pt.

projected wavefunctions for each angular momentum state. The effects of core-polarisation are simulated by ascribing effective charges $e_p=(1+1{\cdot}5\ Z/A)e$ and $e_n=1{\cdot}5\ (Z/A)e$ (Kumar and Baranger 1968) to protons and neutrons respectively. The computed values of $Q(J)$ and $B(E2)$ for each J are shown in tables 1 to 5 for ^{184}Pt, ^{186}Pt, ^{190}Pt, ^{192}Pt and ^{194}Pt, respectively. Unfortunately, the experimental values of $Q(J)$ and $B(E2)$ for these nuclei are scanty in literature. However, as seen from tables 1 to 5, the calculated $B(E2)$ values for the γ-transitions are in good agreement with the corresponding experimental values available in all the nuclei. Special mention can be made for ^{192}Pt and ^{194}Pt where experimental $B(E2)$ values are available up to $J\simeq 8^+$. Our calculated $B(E2)$ values are in fair agreement with the experimental values.

To correlate the Böhr-Mottelson collective model and the microscopic approach followed in this paper, we have calculated the intrinsic quadrupole moment Q^0 from the $Q(J)$ values as well as from the $B(E2)$ values using the following collective model relations:

$$Q(J) = -\frac{J}{2J+3}\,Q_0,$$

$$B(E2;\, J\to J-2) = \frac{15}{32\pi}\,\frac{J(J-1)}{(2J-1)\,(2J+1)}\,Q_0^2.$$

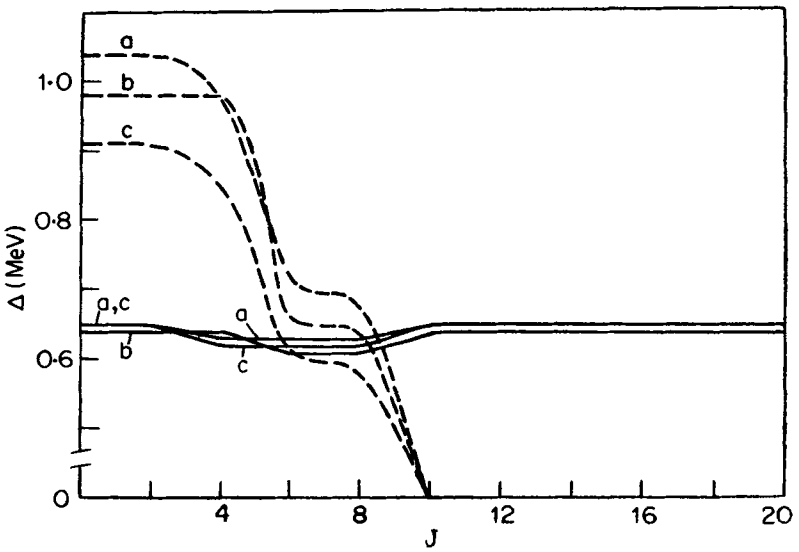

Figure 6. The pairing gaps Δ_p for protons (solid curve) and Δ_n for neutrons (dashed curve) corresponding to the minimum in energy are plotted as function of angular momentum J. The curves a, b, and c refer to ^{190}Pt, ^{192}Pt, and ^{194}Pt respectively.

It is found that in all the nuclei ^{184,186,190,192,194}Pt, the $Q_0(Q)$ extracted from the quadrupole moment $Q(J)$ agrees well with the corresponding $Q_0(E2)$ obtained from $B(E2)$ value for all the angular momentum states J. In general, $Q_0(Q)$ is slightly less than the corresponding $Q_0(E2)$ value, the maximum difference being about 0·1 eb. Our calculations indicate a systematic trend in the behaviour of both Q_0 values as deformation changes for different angular momentum states. We find that in ^{184,186}Pt, the average value of the intrinsic quadrupole moment Q_0 is 4·2 eb for all the states except those with $4 \leqslant J \leqslant 12$ for which the Q_0 value is 4·6 eb. In the case of ^{190,192}Pt, the average value of Q_0 is 4·1 eb for all the states except those with $4 \leqslant J \leqslant 8$ for which the Q_0 value is 4·5 eb and for ^{194}Pt the average value of Q_0 is 3·8 eb for all the states except those with $4 \leqslant J \leqslant 8$ for which the value is 4·2 eb.

4. Conclusions

The microscopic formalism of variation with number conserved projected states is applied to study the high spin yrast states of prolate platinum isotopes ^{184,186}Pt and oblate platinum isotopes ^{190,192,194}Pt. The energy spectra, quadrupole moments and $B(E2)$ values are calculated by employing the nuclear Hamiltonian consisting of quadrupole-plus-pairing interactions. The deformation β, the pairing gaps Δ_p and Δ_n and the chemical potentials λ_p and λ_n are varied simultaneously to obtain the energy minima and to conserve the number of nucleons in each angular momentum state. The effect of core polarisation is simulated by ascribing effective charges to the nucleons and by introducing the moment of inertia of the core to renormalise the energy spectra. The computed $B(E2)$ values and the energy spectra are in fair agreement with the available experimental data. The drastic back-bending observed in ^{190,192,194}Pt at a critical angular momentum $J_c = 10$ can be due to the sudden

vanishing of the neutron pairing gap Δ_n at $J = 10$. The Coriolis decoupling of a neutron pair from the low Ω ($\Omega = 1/2$ and $3/2$) substates of predominantly $i_{13/2}$ orbital in the vicinity of the neutron Fermi surface of these nuclei would also contribute to the observed back-bending in ^{190,192,194}Pt. In ^{184,186}Pt, however, there is no low Ω substate of high j orbit near the neutron Fermi surface and the observed back-bending in these nuclei can only be attributed to the vanishing of the neutron pairing gap at the critical angular momentum.

References

Baktash C, Saladin J X, O'Brien J J and Alessi J G 1978 *Phys. Rev.* **C18** 131

Beshai S, Fransson K, Hjorth S A, Johnson A, Lindblad Th and Sztarkier J 1976 *Z. Phys.* **A277** 351

Cunnane J C, Piipareinen M, Daly P J, Dors C L, Khoo T L and Bernthal F M 1976 *Phys. Rev.* **C13** 2197

Das Gupta S and Gunye M R 1963 *Can. J. Phys.* **42** 762

Davydov A S and Chaban A A 1960 *Nucl. Phys.* **20** 499

Davydov A S and Fillipov G F 1958 *Nucl. Phys.* **8** 237

Faessler A, Greiner W and Sheline R K 1965 *Nucl. Phys.* **70** 33

Faessler A, Grummer F, Lin L and Urbano J 1974 *Phys. Lett.* **B48** 87

Gunye M R, Das Gupta S and Preston M A 1964 *Phys. Lett.* **13** 246

Gunye M R and Warke C S 1979 *J. Phys.* **G5** L83

Grummer F, Schmid K W and Faessler A 1975 *Nucl. Phys.* **A239** 289

Hjorth S A, Johnson A, Lindblad Th, Funke L, Kemnitz P and Winter G 1976 *Nucl. Phys.* **A262** 328

Johnson A and Szymanski Z 1973 *Phys. Rep.* **C7** 181

Johnson N R, Hubert P P, Eichler E, Sarantites D G, Urbon J, Yates S W and Lindblad Th 1977 *Phys. Rev.* **C15** 1325

Kumar K and Baranger M 1968 *Nucl. Phys.* **A110** 529

Mottelson B R and Valatin J G 1960 *Phys. Rev. Lett.* **5** 511

Piiparinen M, Cunnane J C, Daly P J, Dors C L, Bernthal F M and Khoo T L 1975 *Phys. Rev, Lett.* **34** 1110

Richter L, Backe H, Weik F and Willwater R 1979 *Nucl. Phys.* **A319** 221

Sorensen R A 1973 *Rev. Mod. Phys.* **45** 353

Stelzer K, Rauch F, Elze Th, Gould Ch, Idzko J, Mitchell G, Nottrodt H, Zoller R, Wollersheim H and Emling H 1977 *Phys. Lett.* **B70** 297

Sahu R, Satpathy M, Ansari A and Satpathy L 1979 *Phys. Rev.* **C19** 511

Stephens F S and Simon R S 1972 *Nucl. Phys.* **A183** 257

Warke C S and Gunye M R 1975 *Phys. Rev.* **C12** 1647

Warke C S and Gunye M R 1976 *Phys. Rev.* **C13** 859